

# Design and optimization of nonlinear component of block cipher: Applications to multimedia security

Adil Waheed<sup>a</sup>, Fazli Subhan<sup>a,b</sup>, Mazliham Mohd Suud<sup>b,\*</sup>, Muhammad Mansoor Alam<sup>b,c</sup>,  
Sajjad Haider<sup>a</sup>

<sup>a</sup> Faculty of Engineering and Computer Sciences, National University of Modern Languages, Islamabad, Pakistan

<sup>b</sup> Faculty of Computing and Informatics, Multimedia University, Cyberjaya, Malaysia

<sup>c</sup> School of Computer Science in the Faculty of Engineering and IT, University of Technology Sydney, Australia

## ARTICLE INFO

### Keywords:

S-box  
Nonlinear component  
Image encryption  
Nonlinearity  
Security  
Chaotic maps

## ABSTRACT

Nowadays, various image encryption schemes based on chaotic systems have been developed, each of them has its own limitations and strength in terms of security and computational speed. The proposed image encryption scheme utilizes 2-D maps without disturbing their mathematical structure, characterized by topological features such as chaotic behavior and fractal properties, namely the Zaslavsky, Bakers, and Henon Maps. This approach utilizes both confusion and diffusion stages to achieve high levels of security against various attacks. The confusion stage utilizes chaotic values to muddle the rows and columns of the image, reducing the correlations between neighboring pixels, while the diffusion step achieves the avalanche effect with 2D Bakers map and Henon map. The proposed image encryption scheme is analyzed thoroughly to evaluate its security and performance. To evaluate the security and computational efficiency of the proposed image encryption method, various analysis such as correlation, contrast, entropy, energy, homogeneity, and performance analyses are conducted. Moreover, the three proposed S-boxes are also tested to evaluate their effectiveness using cryptographic analysis tests such as nonlinearity, strict Avalanche criterion, differential probability, linear probability, and bit independence criterion, which we also utilized in our proposed image encryption scheme.

## 1. Introduction

The S-box is a fundamental component of a modern block cipher and plays a crucial role in ensuring the security of encrypted communications. S-boxes are designed to provide nonlinear substitution of input data, which helps to dubious the relationship between the plaintext and ciphertext. The S-box is the only nonlinear component of AES, which is one of the most conventional ciphers. Mostly conventional ciphers are not best suited for image encryption due to the unique properties and characteristics of image data [1,2]. Image encryption is entirely different from encryption of textual data because textual data has higher redundancy, which means that encryption algorithms can take advantage of patterns and repetitions. Wang et al. [3] proposed an image encryption scheme based on a laser chaotic system and XOR diffusion, respectively, to achieve rapid transmission and reduce the statistical characteristics of the plain image. The researchers in [4] investigated a color image cryptosystem based on multiple layers fractional-order hyper chaotic map and pseudo random number generator (PRNGs). In

[5], a detailed analytical review regarding construction of nonlinear component is presented. An efficient image encryption algorithm was studied in [6] that combines the shuffling of pixel positions and altering the grayscale values of image pixels to create confusion. By employing PRNG bitstreams generated from cellular automata and the Lorenz system as keys, along with the integration of the S-box, the encryption process achieves well-secured images [7]. The use of PRNGs in image cryptosystems is well-documented in numerous literature examples. The authors of [8] introduced TRNG (True Random Number Generator) based image encryption that relies on the stochastic duration time of double threshold-switching (TS) memristors.

In recent years, there has been a growing interest in using chaotic maps for image encryption due to their ability to produce complex and random sequences that are difficult to predict [9]. Chaotic maps are mathematical functions that exhibit sensitive dependence on initial conditions, which makes them useful for generating random numbers and creating nonlinear transformations that can be used to strengthen cryptographic algorithms [10]. This technique [11] utilizes Arnold's cat

\* Corresponding author.

<https://doi.org/10.1016/j.asej.2023.102507>

Received 9 July 2023; Received in revised form 5 August 2023; Accepted 16 September 2023

Available online 7 October 2023

2090-4479/© 2023 THE AUTHORS. Published by Elsevier BV on behalf of Faculty of Engineering, Ain Shams University. This is an open access article under the CC BY-NC-ND license (<http://creativecommons.org/licenses/by-nc-nd/4.0/>).

**Table 1**

Proposed Chaotic S-box based on modified Zaslavsky May.

|     |     |     |     |     |     |     |     |     |     |     |     |     |     |     |     |
|-----|-----|-----|-----|-----|-----|-----|-----|-----|-----|-----|-----|-----|-----|-----|-----|
| 177 | 202 | 206 | 165 | 158 | 75  | 74  | 39  | 84  | 49  | 216 | 29  | 237 | 207 | 76  | 32  |
| 123 | 115 | 106 | 51  | 219 | 31  | 7   | 145 | 81  | 228 | 33  | 248 | 69  | 182 | 54  | 234 |
| 171 | 112 | 162 | 73  | 110 | 72  | 156 | 92  | 53  | 222 | 173 | 78  | 35  | 9   | 87  | 20  |
| 201 | 225 | 152 | 61  | 160 | 200 | 34  | 132 | 27  | 83  | 241 | 249 | 97  | 62  | 232 | 109 |
| 2   | 42  | 195 | 247 | 233 | 13  | 150 | 103 | 22  | 80  | 120 | 210 | 41  | 95  | 56  | 118 |
| 133 | 211 | 135 | 64  | 91  | 111 | 229 | 180 | 243 | 214 | 127 | 197 | 60  | 90  | 157 | 125 |
| 129 | 37  | 179 | 124 | 235 | 117 | 168 | 43  | 47  | 116 | 227 | 70  | 199 | 164 | 143 | 221 |
| 209 | 178 | 175 | 166 | 17  | 191 | 161 | 192 | 71  | 238 | 185 | 6   | 240 | 104 | 48  | 96  |
| 163 | 100 | 40  | 55  | 138 | 159 | 170 | 236 | 190 | 144 | 1   | 230 | 93  | 67  | 154 | 82  |
| 10  | 139 | 184 | 57  | 217 | 8   | 250 | 28  | 108 | 208 | 186 | 137 | 77  | 0   | 187 | 131 |
| 36  | 231 | 176 | 14  | 167 | 205 | 251 | 148 | 141 | 126 | 11  | 149 | 3   | 25  | 30  | 136 |
| 38  | 215 | 79  | 114 | 169 | 21  | 244 | 52  | 239 | 128 | 66  | 68  | 198 | 119 | 203 | 155 |
| 183 | 255 | 86  | 194 | 140 | 65  | 146 | 130 | 102 | 58  | 212 | 196 | 226 | 85  | 89  | 15  |
| 122 | 220 | 101 | 224 | 105 | 172 | 4   | 46  | 204 | 113 | 245 | 218 | 44  | 88  | 12  | 151 |
| 246 | 193 | 107 | 189 | 50  | 63  | 19  | 23  | 147 | 242 | 252 | 45  | 98  | 174 | 253 | 213 |
| 5   | 94  | 142 | 99  | 254 | 18  | 121 | 16  | 223 | 188 | 24  | 153 | 181 | 59  | 26  | 134 |

map for shuffling of image and also, used cyclic chaos and PRNG as an additional security measure. Chaotic systems have been used for image encryption because they can generate a large amount of random data which can be used as encryption keys or as part of the encryption process. Chaotic systems are also attractive because they are relatively easy to implement and can produce complex and unpredictable behavior. In chaotic image encryption systems, the positions or values of the pixels in the original image are usually exchanged using a chaotic stream cipher. The chaotic stream cipher generates a sequence of random numbers that are used to shuffle the pixels in the image or to modify their values in some way. This process makes it difficult for an attacker to decipher the original image without knowing the encryption key. By incorporating chaotic maps into vulnerable cryptographic schemes, researchers hope to improve their resistance to attacks. Likewise the authors of [12] propose a novel framework for image encryption with the help of two hyperchaotic maps and the single neuron model (SNM). In [13], authors utilized a coset graph to design an S-box with better cryptographic characteristics. Wang et al. [14] presented big data related architecture and general framework which has an ability to collect and store data, including processing, analysis, performance, and security for big data applications. In [15], a comprehensive analysis of blockchain-based applications in the context of security and privacy is presented. Features of gray image are extracted in high frequency domain using multi-resolution multi-direction filtering [16]. This paper [17] presents an optimized approach for cloud provider and its users with better request allocation strategy to reduce energy cost. Lu et al. [18] introduced coupled images decomposition algorithms. These algorithms are robust and accurately restore the images.

In this paper, we propose chaotic based S-boxes using 2-D maps i.e. Zaslavsky map, Honen map and Bakers map. The Zaslavsky is a nonlinear, dynamical and discrete-time system. It produces dynamic and

deterministic behavior which represents an essential part of the encryption algorithms. Moreover, this map is very important it is sensitive to control parameters and can be utilized to create a pseudo-random number generator during the permutation phase. This unique characteristic of sensitivity to control parameters makes it a valuable tool for various cryptographic applications that necessitate randomness [19]. We also propose an S-box using Hénon map. The Hénon map is a two-dimensional discrete-time dynamical system that was introduced by Michel Hénon. It is a simple nonlinear map that exhibits chaotic behavior for certain parameter values. This chaotic behavior can be used in various applications, including image encryption, random number generation, and secure communications. In addition, we constructed an S-box based Baker's map. Currently, Baker's map is being used as a basis for secure communication in stream ciphers. Furthermore, we propose an innovative image encryption algorithm that incorporates each of the proposed S-boxes.

## 2. Preliminaries

The proposed work is based on using 2D chaotic maps, which are mathematical representations of complex systems that exhibit unpredictable and non-repeating behavior for communication of secure data. We drew inspiration from this source [20–22] and acquired knowledge of these algorithms as foundational concepts. This section briefly reviews three chaotic maps, namely the Zaslavsky map, Henon map, and Baker map. Zaslavsky map [21] is a two-dimensional chaotic map that is being used in cryptography. A set of nonlinear equations (1 & 2) define the map, and even for slight modifications to its initial conditions, it behaves in a complex and unpredictable manner. In order to create pseudorandom numbers and create cryptographic algorithms like S-boxes, the Zaslavsky map has been used in different research areas

**Table 2**

S-box derived from modified Henon map.

|     |     |     |     |     |     |     |     |     |     |     |     |     |     |     |     |
|-----|-----|-----|-----|-----|-----|-----|-----|-----|-----|-----|-----|-----|-----|-----|-----|
| 41  | 59  | 187 | 201 | 10  | 221 | 147 | 193 | 163 | 154 | 36  | 38  | 191 | 114 | 246 | 141 |
| 74  | 243 | 98  | 121 | 58  | 153 | 53  | 178 | 228 | 19  | 245 | 215 | 255 | 92  | 203 | 78  |
| 222 | 250 | 34  | 152 | 249 | 133 | 179 | 165 | 168 | 186 | 240 | 69  | 86  | 229 | 97  | 12  |
| 167 | 51  | 83  | 173 | 199 | 218 | 254 | 182 | 55  | 113 | 60  | 16  | 80  | 224 | 183 | 65  |
| 22  | 81  | 110 | 176 | 115 | 91  | 251 | 211 | 26  | 219 | 45  | 161 | 140 | 57  | 162 | 238 |
| 137 | 207 | 210 | 216 | 71  | 117 | 101 | 61  | 31  | 24  | 205 | 151 | 73  | 190 | 47  | 66  |
| 202 | 135 | 46  | 50  | 148 | 119 | 40  | 177 | 170 | 122 | 233 | 100 | 2   | 84  | 33  | 105 |
| 39  | 129 | 220 | 4   | 127 | 52  | 169 | 208 | 252 | 14  | 164 | 54  | 144 | 62  | 21  | 64  |
| 76  | 209 | 37  | 17  | 150 | 241 | 189 | 13  | 156 | 108 | 149 | 239 | 118 | 204 | 155 | 213 |
| 235 | 244 | 206 | 67  | 226 | 212 | 116 | 126 | 146 | 192 | 124 | 0   | 42  | 1   | 232 | 188 |
| 128 | 35  | 175 | 227 | 120 | 111 | 225 | 43  | 3   | 56  | 25  | 194 | 214 | 109 | 236 | 130 |
| 15  | 248 | 94  | 185 | 72  | 231 | 70  | 20  | 230 | 145 | 157 | 132 | 196 | 88  | 63  | 123 |
| 103 | 77  | 49  | 99  | 89  | 28  | 85  | 112 | 7   | 87  | 75  | 198 | 242 | 44  | 160 | 181 |
| 79  | 142 | 139 | 174 | 159 | 90  | 166 | 106 | 107 | 18  | 11  | 247 | 95  | 200 | 172 | 27  |
| 68  | 180 | 93  | 234 | 32  | 5   | 143 | 48  | 138 | 171 | 30  | 195 | 217 | 158 | 253 | 136 |
| 184 | 104 | 134 | 237 | 102 | 125 | 223 | 96  | 82  | 131 | 8   | 9   | 29  | 23  | 197 | 6   |

**Table 3**

S-box construction based on modified Baker's Map.

|     |     |     |     |     |     |     |     |     |     |     |     |     |     |     |     |
|-----|-----|-----|-----|-----|-----|-----|-----|-----|-----|-----|-----|-----|-----|-----|-----|
| 121 | 159 | 190 | 82  | 146 | 6   | 104 | 156 | 223 | 161 | 76  | 63  | 236 | 244 | 115 | 43  |
| 20  | 51  | 102 | 84  | 133 | 28  | 141 | 10  | 66  | 155 | 196 | 178 | 3   | 211 | 30  | 172 |
| 45  | 242 | 234 | 147 | 125 | 5   | 170 | 93  | 41  | 78  | 217 | 39  | 127 | 228 | 74  | 145 |
| 238 | 226 | 54  | 55  | 37  | 169 | 142 | 221 | 80  | 75  | 230 | 52  | 33  | 116 | 67  | 9   |
| 213 | 106 | 222 | 214 | 165 | 180 | 198 | 31  | 212 | 204 | 19  | 70  | 56  | 252 | 235 | 2   |
| 192 | 69  | 42  | 50  | 149 | 123 | 117 | 135 | 22  | 195 | 247 | 77  | 25  | 219 | 233 | 203 |
| 194 | 29  | 44  | 72  | 249 | 4   | 58  | 124 | 245 | 96  | 81  | 60  | 32  | 250 | 103 | 88  |
| 87  | 216 | 85  | 182 | 181 | 90  | 97  | 237 | 1   | 14  | 11  | 86  | 23  | 21  | 166 | 160 |
| 240 | 38  | 184 | 140 | 188 | 35  | 26  | 100 | 71  | 62  | 24  | 251 | 200 | 113 | 129 | 79  |
| 187 | 0   | 8   | 138 | 255 | 227 | 136 | 218 | 132 | 205 | 61  | 224 | 120 | 119 | 175 | 130 |
| 110 | 49  | 254 | 46  | 99  | 57  | 114 | 131 | 207 | 95  | 27  | 73  | 36  | 7   | 153 | 191 |
| 168 | 64  | 157 | 109 | 177 | 48  | 183 | 47  | 15  | 108 | 68  | 134 | 101 | 232 | 248 | 128 |
| 118 | 151 | 253 | 199 | 163 | 34  | 137 | 17  | 189 | 229 | 246 | 94  | 162 | 152 | 12  | 243 |
| 201 | 98  | 208 | 241 | 220 | 206 | 107 | 210 | 16  | 209 | 83  | 193 | 122 | 158 | 167 | 105 |
| 239 | 143 | 65  | 13  | 144 | 202 | 174 | 59  | 197 | 126 | 171 | 176 | 112 | 173 | 186 | 179 |
| 53  | 148 | 111 | 139 | 225 | 231 | 18  | 215 | 164 | 91  | 92  | 154 | 89  | 150 | 185 | 40  |

**Table 4**

Experimental Results and Comparison with known S-boxes.

| S-box                   | Nonlinearity |            |               | SAC           | BIC-NL        | BIC-SAC       | DP        | LP            |
|-------------------------|--------------|------------|---------------|---------------|---------------|---------------|-----------|---------------|
|                         | MaxVal       | MinVal     | AvrVal        | AvrVal        | AvrVal        | AvrVal        | MaxVal    | MaxVal        |
| Abd-El-Atty [26]        | 106          | 98         | 101.50        | 0.5043        | 104.28        | 0.5071        | 12        | 0.125         |
| Zhu [27]                | 108          | 102        | 105.75        | 0.5021        | 104.14        | 0.5050        | 10        | 0.1328        |
| Zahid [28]              | 112          | 110        | 111.75        | 0.5029        | 103.74        | 0.5005        | 10        | 0.125         |
| Alghafis [29]           | 105          | 97         | 102.87        | 0.5192        | 102.67        | 0.4787        | 54        | 0.1679        |
| Jiang [30]              | 108          | 104        | 106.75        | 0.4975        | 103.57        | 0.5022        | 10        | 0.1328        |
| Dimitrov [31]           | 114          | 116        | 114.50        | 0.5012        | 104.21        | 0.5046        | 10        | 0.1406        |
| Shahzad [32]            | 112          | 108        | 110.50        | 0.5031        | 109.21        | 0.5018        | 6         | 0.0859        |
| Hua [33]                | 108          | 102        | 105.25        | 0.5351        | 103.25        | 0.5087        | –         | 0.1406        |
| Javeed [34]             | 110          | 106        | 107.50        | 0.4997        | 104.64        | 0.5048        | 12        | 0.1406        |
| Ali [35]                | 106          | 98         | 102.75        | 0.4992        | 103.07        | 0.0140        | 12        | 0.1406        |
| Hematpour [36]          | 109          | 102        | 105.25        | 0.4960        | 104.53        | 0.5045        | –         | 0.1328        |
| Nizam Chew [37]         | 112          | 112        | 112.00        | 0.4980        | 112.00        | 0.4981        | 4         | 0.0625        |
| Artuğer [38]            | 112          | 110        | 111.75        | 0.4968        | 104.00        | 0.5016        | 12        | 0.125         |
| <b>Proposed S-box-1</b> | <b>116</b>   | <b>116</b> | <b>113.75</b> | <b>0.4956</b> | <b>103.42</b> | <b>0.4992</b> | <b>10</b> | <b>0.1406</b> |
| <b>Proposed S-box-2</b> | <b>112</b>   | <b>116</b> | <b>114.25</b> | <b>0.4978</b> | <b>103.41</b> | <b>0.5044</b> | <b>10</b> | <b>0.125</b>  |
| <b>Proposed S-box-3</b> | <b>112</b>   | <b>112</b> | <b>112</b>    | <b>0.5063</b> | <b>103.86</b> | <b>0.4987</b> | <b>10</b> | <b>0.1328</b> |

[23]. Henon map [22] is a two dimensional map that exhibits chaotic behavior. The Henon map has been widely used as building block for cryptographic primitives due its chaotic behavior, such as construction of nonlinear component of block cipher and stream ciphers [24,25]. It is defined by following two nonlinear equations (Eq. 3 & 4) and maps each point in a 2-D plane to a new point. Whereas, the Baker's is also a 2-D map [20] that has been used in cryptography, image processing, signal processing, and encryption applications because of its sensitivity to initial conditions and its capacity to generate pseudo random numbers. The Baker's map is used to map square grid of points onto itself. It is described by a set of recurrence equations that iteratively transform the coordinates of every grid point.

### 3. Proposed S-box scheme

In this article, we propose a novel S-box design and image encryption scheme that utilize chaotic maps, specifically the Zaslavas, Bakers, and Henon maps. These maps are known for their chaotic behavior and sensitivity to initial conditions, which make them useful for generating pseudo-random sequences that can be used in cryptographic applications. Our generated S-boxes meet all relevant standards and exhibit impressive results in analysis (see Tables 1–4), including nonlinearity (NL), Strict Avalanche Criterion (SAC), Bit Independence Criterion (BIC), LP (linear probability), and DP (Differential probability).

#### 3.1. Modified Zaslavsky map, Henon Map, and Baker's map based nonlinear component construction without disturbing their mathematica structure

The proposed scheme of the Zaslavsky map algorithm involves a series of well-defined steps to generate pseudorandom numbers (PRNs). The process starts with initializing the variables to some predetermined values, which are then used to calculate the parameter  $\mu$ .

Once  $\mu$  is determined, a loop is initiated to perform a 2 million (2,000,000) iterations. Within this loop, the Zaslavsky map equations are used to generate the new values of  $x$  and  $y$ , which are then used to calculate four PRNs. These PRNs are printed in decimal and binary form, and the values of  $x$  and  $y$  are updated to their new values for the next iteration of the loop. The algorithm can be repeated with variations to generate longer sequences of PRNs. The strength of this algorithm lies in its chaotic nature, which makes it difficult for an adversary to predict the sequence of PRNs generated.

The following is an algorithm based on Zaslavsky map for generating resistant to cryptanalysis nonlinear component of block Cipher.

##### Algorithm-1: Proposed S-box construction Algorithm-1

**Step 1.** Initialize variables  $x, y, v, e, \tau$  and size with some specific required values.

**Step 2.** Calculate the value of  $\mu$  using the formula  $1 - e^{-\tau}/\tau$ .

**Step 3.** While (size  $\leq$  2,000,000).

**Step 3.1.** Calculate the new values of  $x_1$  and  $y_1$  using the chaotic map equations:

$$x_1 = \text{mod}(y_n + v(1 + \mu z_n) + \epsilon v \mu z_n \cos(2\pi y_n), 1)$$

$$y_1 = e^{-\tau}(z_n + \cos(2\pi y_n))$$

**Step 3.2.** Calculate pseudo random number for S-box design

(continued on next page)

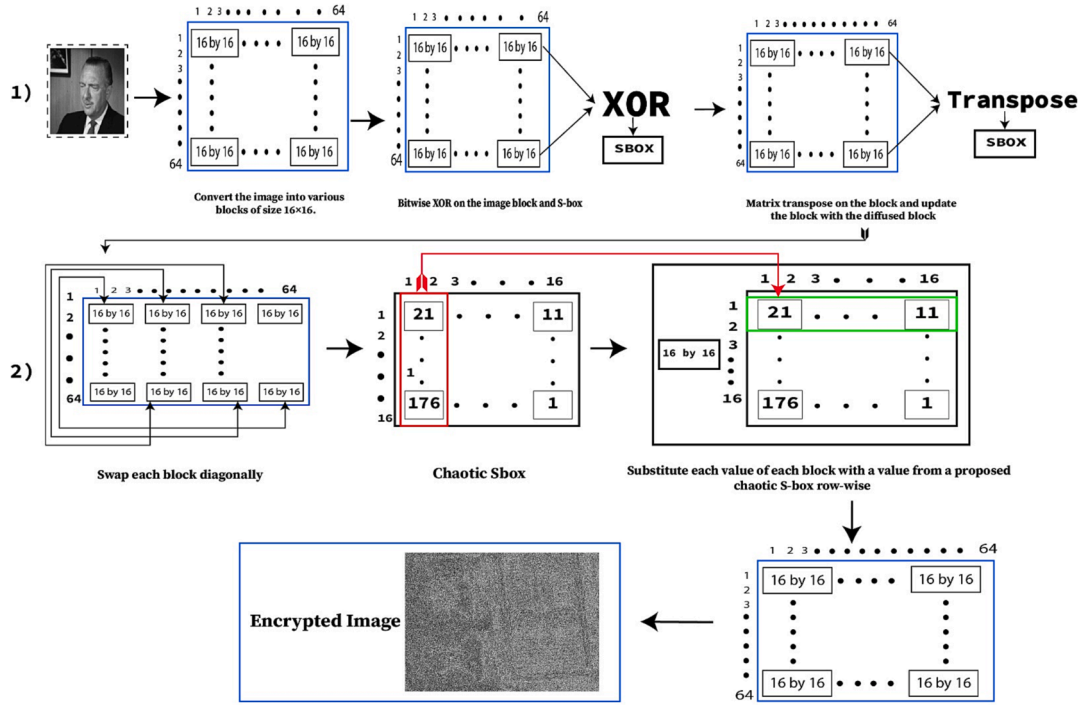


Fig. 1. A pictorial view of an image encryption algorithm.

(continued)

**Algorithm-1:** Proposed S-box construction Algorithm-1

```

prn = mod(floor( $x_1 \times (2^{42}-1)$ ), 256)
binaryNo = convert(prn) ▷ This function will convert the PRN into binary number
firstComp = complementCal(binaryNo) ▷ The function calculates first complement
XORingResult ← ApplyXORbetweenfirstCompande
SboxArray ← XORedvaluedisstoredintheSboxArrayatthecorrespondingindex
Step 4. End of while loop
Step 7. To construct reliable S-box, apply permutation to the newly generated pseudo
random numbers.

```

(continued)

**Algorithm 2:** Proposed S-box design algorithm-2

```

Step 3.4.3. For each position, flip the binary representation.
Step 3.4.4. Reverse the binary representation and return the result in decimal
form.
Step 3.4.5. Change the bits in the original position to match the bits in the
reversed position.
Step 3.4.6. Store the resultant value into SboxArray.
Step 4. End of ForEach loop
Step 9. Organize the resulting values into a 16 × 16S-box for cryptosystems.

```

The proposed algorithm below commences by setting the initial values of  $x$  and  $y$ , as well as the values for  $a$ ,  $b$ , and the total number of iterations to be carried out. The Henon map is iterated 1.5 million times (1,500,000) to generate unpredictable values of  $x$  and  $y$ , which are utilized to calculate a new value of  $x$ . This value is then multiplied by a specific value and rounded down to produce a pseudorandom number. This random number is constrained to a value between 0 and 255 by computing its modulus with 256. This process is repeated iteratively until we get desired bijective values, and the resulting values are organized into a  $16 \times 16$ S-box.

The following is an algorithm to generate secure S-box using Henon Map:

**Algorithm 2:** Proposed S-box design algorithm-2

```

Step 1. Set the initial values of  $x$  and  $y$ .
Step 2. Set the values of  $a$ ,  $b$ , and size.
Step 3. FOREACH 1:1,500,000.
 $x_{n+1} = 1 + y_n - ax_n^2$ 
 $y_{n+1} = bx_n$ 
Step 3.1. Print the chaotic values of  $x_1$  and  $y_1$ .
Step 3.2. For each new value of  $x_1$ , multiply it by  $(2^{35}-1)$  and floor it.
 $prn = \text{floor}(x_1 \times (2^{35}-1))$ 
Step 3.3. Take the modulus of pseudorandom number with 256 to get a value
between 0 and 255.
Step 3.4. Apply following bit shuffling permutation on PRN
Step 3.4.1. convert PRN into binary
Step 3.4.1.1. Take the binary sequence of length N
Step 3.4.2. Represent each bit's position in binary form.

```

(continued on next column)

The Baker's map design an S-box by defining the parameters  $a$ ,  $size$ ,  $x$ ,  $y$ , and required arrays. Subsequently, unpredictable values of  $x$  and  $y$  are generated by Henon map. The two different branches of the this map modify the values  $x$  and  $y$ . These modified values are stored into  $xSboxkey$  and  $ySboxkey$  arrays, respectively. Chaotic values of S-box are actually floating point numbers. These numbers are multiplied with any specific number and take modulo with 256 to constraint the values in range of 0 to 255. The following is a procedure to construct an S-box using Baker's map.

**Algorithm 3:** S-box derived from modified Baker's map

```

Step 1. Define the parameters and initializes required arrays with zeros.
Step 2. For Loop from 1 to rang (2,000,000)
Step 2.1. If  $0 < x \leq 0.5$  ←update  $x$  and  $y$  according to the first branch of the
map
 $x \leftarrow 2 * x$ 
 $y \leftarrow a * y$ 
Step 2.2. If  $0.5 < x \leq 1$  ←update  $x$  and  $y$  according to the second branch of the
map
 $x \leftarrow 2 * x - 1$ ,
 $y \leftarrow a * y + 0.5$ 
Step 6. Store the updated values of  $x$  and  $y$  into  $xSboxkey$  and  $ySboxkey$  arrays,
respectively.
Step 7. Multiply each value of  $xSboxkey$  arrays with specific number then take mod
with 256 to constraint values between 0 and 255.
Step 8. Convert updated  $xSboxkey$  into corresponding 8-bit binary number.
Step 9. Define 8-bit binary constant (key) for addition-based hash permutation.
Step 10. Add the updated  $xSboxkey$  and the key together (modulo 256).
Step 11. Store the resultant value into SboxArray

```

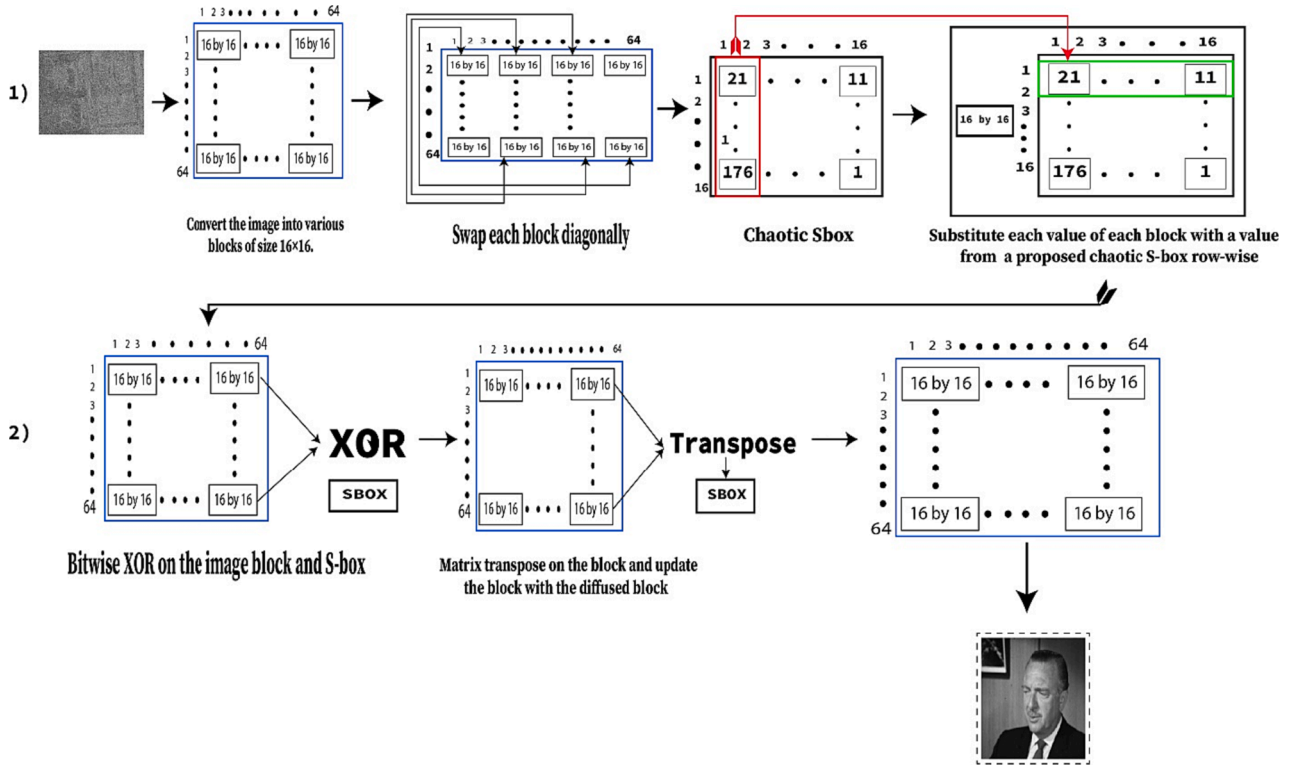


Fig. 2. A pictorial view of an image decryption algorithm.

#### 4. Proposed image encryption algorithm

Both one dimensional (1-D) and two dimensional (2-D) maps are used in the field of cryptography. Generally, 1-D maps are used to generate encryption keys or digital signatures but the issue is that generated keys with 1-D maps are small in size and have lower degree of complexity and randomness. However, 2-D maps are considered more secure due to larger key size, parameters, space, and complexity. That's the reason we employed 2-D maps (Zaslavsky, Henon, Bakers). These maps reached a chaotic state to provide nonlinear and dynamical behavior.

In this image encryption algorithm, initially, an assessment is conducted to determine whether the image is grayscale or RGB. In case of RGB, the image is transformed into a grayscale. Next, a verification is made to determine whether the dimensions of the image are divisible by 16, if it is not then in this case, pad the image with some extra pixels on the sides until the width and height are both divisible by 16. The following is an algorithm to solve perfect division issue:

- Read and calculate the actual height and width of the image.
- Find the multiples of 16 that are closest (greater) to or equal to the current height and width. Assign the names 'new\_height' and 'new\_width' to these new values.
- Subtract the actual height and width from 'new\_height' and 'new\_width'
- Create the blank canvas with new\_height and new\_width.
- Copy the original image to the center of canvas
- Padding the remaining area with white pixels.
- The padding image is perfectly divisible by 16.

Once the image has been subdivided into  $16 \times 16$  blocks, a swapping process is conducted whereby the upper diagonal of the first block is swapped with the lower diagonal of the last block, the lower diagonal of first block is swapped with upper diagonal of last block and vice versa.

This process is repeated for each block in the image. After the completion of the swapping process, perform row-wise substitution on each value of each block with value of proposed chaotic S-box to encrypt the image (See Fig. 1). The following is the novel image encryption algorithm based on the proposed chaotic S-boxes.

##### Algorithm 4: Proposed Image Encryption Scheme

- Step 1. Read the original image and examine its dimensions.
- Step 2. Check whether the image is Grayscale or RGB.
- Step 3. If the image is RGB, convert it into a Grayscale image.
- Step 4. Check if the image is divisible into  $16 \times 16$  blocks.
- Step 5. If the image is not divisible into  $16 \times 16$  blocks, add padding (white pixels) to make an image size divisible by 16.
- Step 6. Convert the image into various blocks of size  $16 \times 16$ . Each block individually reveals no information about the plain image.
- Step 7. Apply a confusion layer to each block, i.e., perform a bitwise XOR on the image block and S-box and update the block with the confused block.
- Step 8. Apply a diffusion layer to each block i.e., perform matrix transpose on the block and update the block with the diffused block.
- Step 9. Perform multiple rounds of the confusion layer and diffusion layer to enhance the encryption strength and ensure better dispersion of pixel values.
- Step 10. Swap each block diagonally to further muddle the number of rows and columns and introduce additional confusion.
- Step 11. Substitute each value of each block with a value from a proposed chaotic S-box row-wise, using a lookup operation based on the S-box table.
- Step 12. Repeat Steps 7 to 11 for a desired number of rounds.
- Step 13. Finally, the image is encrypted, and the encrypted image is obtained.

Additionally, we selected an image block of size  $16 \times 16$  due to following reasons:

- In our proposed image encryption algorithm, we use an Substitution Box (S-box) of size  $16 \times 16$ , which is a well-known and standard size.
- The image block of size  $16 \times 16$  provides a good balance between cryptographic strength and computational efficiency. This size guarantees robust nonlinearity, resistance to linear and differential cryptanalysis, and compatibility with modern cryptographic algorithms.



**Table 5**  
Nonlinearity for Proposed S-boxes.

| Proposed S-boxes | Nonlinearity:                |     |     |     |     |     |     |     |
|------------------|------------------------------|-----|-----|-----|-----|-----|-----|-----|
|                  | 0                            | 1   | 2   | 3   | 4   | 5   | 6   | 7   |
| Proposed S-box-1 | 114                          | 114 | 114 | 112 | 112 | 116 | 112 | 116 |
|                  | Average Nonlinearity: 113.75 |     |     |     |     |     |     |     |
| Proposed S-box-2 | 112                          | 114 | 114 | 114 | 114 | 116 | 114 | 116 |
|                  | Average Nonlinearity: 114.25 |     |     |     |     |     |     |     |
| Proposed S-box-3 | 112                          | 112 | 112 | 112 | 112 | 112 | 112 | 112 |
|                  | Average Nonlinearity: 112    |     |     |     |     |     |     |     |

#### 4.1. Image decryption algorithm

In order to decrypt the image, each step must be carried out in reverse order, exactly as it was done during the encryption process. This process ensures that original image is recreated perfectly (see Fig. 2). Here are the steps to decrypt an encrypted image.

##### Algorithm 5: Image Decryption Scheme

- Step 1.** Read the encrypted image and examine its dimensions.
- Step 2.** Reverse the row-wise substitution process by swapping each entry of each block with the chaotic S-box.
- Step 3.** Diagonally swap each block of the encrypted image.
- Step 4.** To reverse the diffusion process, transpose each block back to its original form.
- Step 5.** Undo the confusion operation by performing XOR between each block of encrypted image and chaotic S-box.
- Step 5.** To recreate the original image, reassemble the decrypted blocks back together.
- Step 6.** To get the actual dimensions of the decrypted image, remove the zero padding.
- Step 7.** If the original image was converted from RGB to grayscale, the decrypted image is restored to its original color format.
- Step 9.** Finally, the image is decrypted back to its original form.

## 5. Performance analysis of proposed chaotic S-boxes

In order to analyze the cryptographic properties of proposed chaotic S-boxes, we perform bijectivity, Strict Avalanche criterion (SAC), nonlinearity (NL), BIC (Bit Independence Criterion), linear probability (LP), and Differential probability (DP) measurement criteria. We also examine resistance of chaotic S-boxes against linear and differential attacks.

#### 5.1. Nonlinearity

Linearity is viewed as a curse in the field of cryptography because it makes system vulnerable to attacks. In contrast, nonlinearity ensures that the output of cryptographic system is not a linear combination of its vectors. If an S-box has linear mapping between its input and output, its resistance level is very low [39]. So, nonlinearity is a metric to assess the level of confusion and diffusion provided by the S-box. It refers to the degree to which the output bits of an S-box (nonlinear component of block cipher) are dependent on its input bits. In other words, a high degree of nonlinearity makes it challenging for an attacker to predict the S-box's output from its input. AES S-box has nonlinearity 112 which

provides good resistance against linear and differential attacks. It is pertinent to mention that nonlinearity results of our proposed S-boxes are better than AES, as shown in Table 5 below.

$$N_{\theta} = 2^{n-1} - \frac{1}{2} \left[ \left( h \in GF(2)^{n_{max}} \right) |S_{\theta}(h)| \right] \quad (6)$$

$$S_{\theta}(h) = \sum_{g \in GF(2)^n} (-1)^{\theta(g) \oplus g \cdot h} \quad (7)$$

#### 5.2. Strict avalanche criterion

The strict avalanche criterion (SAC) measures the sensitivity of S-box to small possible change in its input. This criterion quantifies how much the output of an S-box changes when a single input bit is flipped. The result of an S-box satisfying this property is that each output bit will change with a probability that is close to 0.5 [40], so this value examine that the SAC is suitable property for measuring the sensitivity of S-box. We examine our three proposed S-boxes as shown in (see Tables 6–8). The average results of SAC are near to 0.5, which indicates that criterion is satisfied .

#### 5.3. Bit independence criteria (BIC)

BIC is an another criterion to evaluate the cryptographic properties of an S-box. BIC is a metric used to assess how statistically output bits of an S-box are independent from its input bits [41]. A BIC value that is close to zero means that the S-box has strong bit independence and thus offers good diffusion. In case the value of BIC is significantly greater than zero, which indicates S-box is not statistically independent and may be vulnerable to attacks. Here are the BIC results Tables 9–11 of the proposed S-boxes while comparing them with well-known S-boxes.

#### 5.4. Differential approximation probability

The differential approximation probability ( $DP_f$ ) refers that a Boolean function will produce a particular value in response to a change in its input. This change represents XOR distribution between input and output. The input is represented by  $\Delta x$  and the output is denoted as  $\Delta y$ . The formula to calculate differential probability is given as follows:

$$DP_f = \max_{\Delta x \neq 0, \Delta y} \left( \frac{|\{x \in X | f(x) \oplus f(x \oplus \Delta x) = \Delta y\}|}{2^n} \right) \quad (8)$$

Where  $2^n$  represents the number of elements in the set,  $X$  represents a set of all possible inputs. The value of  $DP_f$  affects how well the S-box defends against differential attacks. The S-box is regarded as having strong defenses against these attacks if  $DP_f$  is small. On the other hand, if  $DP_f$  is large, it is thought that the S-box is incapable of fending off such attacks. The following are the differential probability results for our proposed S-boxes (see Table 12).

**Table 6**  
SAC Results for S-box-1.

| Strict Avalanche Criterion: |                      |         |         |         |         |         |         |         |
|-----------------------------|----------------------|---------|---------|---------|---------|---------|---------|---------|
| SAC for Proposed S-box-1    | 0                    | 1       | 2       | 3       | 4       | 5       | 6       | 7       |
|                             | 0.59375              | 0.48438 | 0.46875 | 0.53125 | 0.54688 | 0.51563 | 0.46875 | 0.50000 |
|                             | 0.48438              | 0.51563 | 0.50000 | 0.53125 | 0.46875 | 0.48438 | 0.46875 | 0.53125 |
|                             | 0.48438              | 0.48438 | 0.48438 | 0.45313 | 0.45313 | 0.46875 | 0.48438 | 0.50000 |
|                             | 0.50000              | 0.59375 | 0.54688 | 0.50000 | 0.51563 | 0.46875 | 0.53125 | 0.42188 |
|                             | 0.45313              | 0.42188 | 0.51563 | 0.46875 | 0.43750 | 0.51563 | 0.56250 | 0.46875 |
|                             | 0.46875              | 0.50000 | 0.46875 | 0.53125 | 0.48438 | 0.45313 | 0.48438 | 0.53125 |
|                             | 0.48438              | 0.45313 | 0.53125 | 0.51563 | 0.50000 | 0.53125 | 0.46875 | 0.46875 |
|                             | 0.50000              | 0.50000 | 0.46875 | 0.51563 | 0.50000 | 0.50000 | 0.53125 | 0.50000 |
|                             | Average SAC: 0.49560 |         |         |         |         |         |         |         |

**Table 7**  
SAC results for S-box-2.

| SAC for Proposed S-box-2 | 0       | 1       | 2       | 3       | 4       | 5       | 6       | 7       |
|--------------------------|---------|---------|---------|---------|---------|---------|---------|---------|
|                          | 0.57813 | 0.48438 | 0.54688 | 0.48438 | 0.56250 | 0.50000 | 0.46875 | 0.45313 |
|                          | 0.50000 | 0.50000 | 0.56250 | 0.56250 | 0.51563 | 0.53125 | 0.46875 | 0.50000 |
|                          | 0.43750 | 0.48438 | 0.46875 | 0.46875 | 0.51563 | 0.48438 | 0.51563 | 0.46875 |
|                          | 0.46875 | 0.51563 | 0.43750 | 0.43750 | 0.48438 | 0.51563 | 0.51563 | 0.56250 |
|                          | 0.54688 | 0.50000 | 0.46875 | 0.48438 | 0.56250 | 0.51563 | 0.53125 | 0.46875 |
|                          | 0.48438 | 0.45313 | 0.48438 | 0.53125 | 0.46875 | 0.50000 | 0.46875 | 0.53125 |
|                          | 0.48438 | 0.45313 | 0.45313 | 0.45313 | 0.53125 | 0.46875 | 0.46875 | 0.53125 |
|                          | 0.50000 | 0.50000 | 0.53125 | 0.50000 | 0.50000 | 0.50000 | 0.46875 | 0.51563 |
| Average SAC: 0.49780     |         |         |         |         |         |         |         |         |

**Table 8**  
SAC Results for S-box-3.

| SAC Proposed S-box-3 | 0       | 1       | 2       | 3       | 4       | 5       | 6       | 7       |
|----------------------|---------|---------|---------|---------|---------|---------|---------|---------|
|                      | 0.46875 | 0.50000 | 0.45313 | 0.50000 | 0.57813 | 0.48438 | 0.53125 | 0.56250 |
|                      | 0.50000 | 0.48438 | 0.46875 | 0.45313 | 0.48438 | 0.50000 | 0.51563 | 0.54688 |
|                      | 0.46875 | 0.56250 | 0.46875 | 0.50000 | 0.53125 | 0.48438 | 0.51563 | 0.42188 |
|                      | 0.50000 | 0.48438 | 0.54688 | 0.43750 | 0.50000 | 0.57813 | 0.57813 | 0.56250 |
|                      | 0.48438 | 0.51563 | 0.46875 | 0.50000 | 0.48438 | 0.51563 | 0.53125 | 0.53125 |
|                      | 0.54688 | 0.45313 | 0.48438 | 0.53125 | 0.56250 | 0.54688 | 0.50000 | 0.45313 |
|                      | 0.54688 | 0.45313 | 0.54688 | 0.51563 | 0.50000 | 0.50000 | 0.57813 | 0.50000 |
|                      | 0.46875 | 0.51563 | 0.48438 | 0.54688 | 0.50000 | 0.45313 | 0.51563 | 0.50000 |
| Average SAC: 0.50634 |         |         |         |         |         |         |         |         |

**Table 9**  
BIC for Proposed S-box-1.

| BIC for Proposed S-box-1 | 0        | 1        | 2        | 3        | 4        | 5        | 6        | 7        |
|--------------------------|----------|----------|----------|----------|----------|----------|----------|----------|
|                          | —        | 0.505859 | 0.511719 | 0.503906 | 0.507812 | 0.486328 | 0.492188 | 0.492188 |
|                          | 0.505859 | —        | 0.503906 | 0.505859 | 0.490234 | 0.523438 | 0.490234 | 0.496094 |
|                          | 0.511719 | 0.503906 | —        | 0.513672 | 0.474609 | 0.505859 | 0.490234 | 0.496094 |
|                          | 0.503906 | 0.505859 | 0.513672 | —        | 0.517578 | 0.494141 | 0.478516 | 0.513672 |
|                          | 0.507812 | 0.490234 | 0.474609 | 0.517578 | —        | 0.490234 | 0.494141 | 0.500000 |
|                          | 0.486328 | 0.523438 | 0.505859 | 0.494141 | 0.490234 | —        | 0.498047 | 0.500000 |
|                          | 0.492188 | 0.490234 | 0.490234 | 0.478516 | 0.494141 | 0.498047 | —        | 0.501953 |
|                          | 0.492188 | 0.496094 | 0.496094 | 0.513672 | 0.500000 | 0.500000 | 0.501953 | —        |
| Average BIC: 0.49923     |          |          |          |          |          |          |          |          |

**Table 10**  
BIC for Proposed S-box-2.

| BIC for Proposed S-box-2 | 0        | 1        | 2        | 3        | 4        | 5        | 6        | 7        |
|--------------------------|----------|----------|----------|----------|----------|----------|----------|----------|
|                          | —        | 0.498047 | 0.519531 | 0.507812 | 0.500000 | 0.494141 | 0.503906 | 0.488281 |
|                          | 0.498047 | —        | 0.511719 | 0.492188 | 0.529297 | 0.527344 | 0.507812 | 0.507812 |
|                          | 0.519531 | 0.511719 | —        | 0.494141 | 0.496094 | 0.501953 | 0.496094 | 0.498047 |
|                          | 0.507812 | 0.492188 | 0.494141 | —        | 0.513672 | 0.507812 | 0.496094 | 0.515625 |
|                          | 0.500000 | 0.529297 | 0.496094 | 0.513672 | —        | 0.496094 | 0.519531 | 0.494141 |
|                          | 0.494141 | 0.527344 | 0.501953 | 0.507812 | 0.496094 | —        | 0.492188 | 0.500000 |
|                          | 0.503906 | 0.507812 | 0.496094 | 0.496094 | 0.519531 | 0.492188 | —        | 0.515625 |
|                          | 0.488281 | 0.507812 | 0.498047 | 0.515625 | 0.494141 | 0.500000 | 0.515625 | —        |
| Average BIC: 0.01026     |          |          |          |          |          |          |          |          |

**Table 11**  
BIC for Proposed S-box-3.

| BIC for Proposed S-box-3 | —        | 0.484375 | 0.478516 | 0.5      | 0.503906 | 0.494141 | 0.519531 | 0.513672 |
|--------------------------|----------|----------|----------|----------|----------|----------|----------|----------|
|                          | 0.484375 | —        | 0.496094 | 0.505859 | 0.503906 | 0.482422 | 0.492188 | 0.496094 |
|                          | 0.478516 | 0.496094 | —        | 0.521484 | 0.503906 | 0.501953 | 0.474609 | 0.480469 |
|                          | 0.5      | 0.505859 | 0.521484 | —        | 0.478516 | 0.507812 | 0.521484 | 0.523438 |
|                          | 0.503906 | 0.503906 | 0.503906 | 0.478516 | —        | 0.490234 | 0.501953 | 0.498047 |
|                          | 0.494141 | 0.482422 | 0.501953 | 0.507812 | 0.490234 | —        | 0.498047 | 0.490234 |
|                          | 0.519531 | 0.492188 | 0.474609 | 0.521484 | 0.501953 | 0.498047 | —        | 0.5      |
|                          | 0.513672 | 0.496094 | 0.480469 | 0.523438 | 0.498047 | 0.490234 | 0.5      | —        |
| Average BIC: 0.01256     |          |          |          |          |          |          |          |          |

**Table 12**

DP for Proposed S-boxes.

| 0  | 1 | 2  | 3 | 4  | 5  | 6 | 7  | 8  | 9 | 10 | 11 | 12 | 13 | 14 | 15 |
|----|---|----|---|----|----|---|----|----|---|----|----|----|----|----|----|
| 0  | 6 | 6  | 8 | 8  | 6  | 6 | 8  | 6  | 6 | 8  | 10 | 8  | 6  | 6  | 6  |
| 8  | 8 | 8  | 8 | 8  | 6  | 6 | 8  | 6  | 6 | 6  | 6  | 6  | 8  | 8  | 6  |
| 8  | 6 | 6  | 6 | 8  | 6  | 6 | 8  | 6  | 6 | 6  | 6  | 8  | 8  | 6  | 6  |
| 8  | 8 | 8  | 8 | 8  | 6  | 6 | 6  | 6  | 6 | 8  | 6  | 6  | 6  | 6  | 6  |
| 6  | 8 | 8  | 6 | 8  | 6  | 8 | 8  | 6  | 6 | 6  | 8  | 8  | 6  | 8  | 6  |
| 6  | 8 | 6  | 8 | 6  | 6  | 8 | 8  | 8  | 6 | 10 | 8  | 6  | 6  | 6  | 6  |
| 6  | 6 | 8  | 6 | 6  | 8  | 4 | 6  | 8  | 8 | 6  | 8  | 6  | 8  | 8  | 6  |
| 10 | 8 | 6  | 6 | 6  | 6  | 8 | 8  | 8  | 8 | 8  | 8  | 6  | 8  | 6  | 10 |
| 6  | 6 | 8  | 8 | 10 | 8  | 8 | 6  | 8  | 6 | 8  | 6  | 6  | 8  | 10 | 6  |
| 6  | 8 | 6  | 6 | 6  | 8  | 6 | 8  | 8  | 6 | 6  | 6  | 6  | 6  | 8  | 8  |
| 6  | 8 | 6  | 6 | 8  | 8  | 6 | 10 | 6  | 6 | 8  | 8  | 6  | 6  | 6  | 8  |
| 6  | 6 | 6  | 6 | 8  | 6  | 8 | 6  | 6  | 6 | 6  | 8  | 6  | 6  | 6  | 8  |
| 6  | 6 | 6  | 6 | 6  | 10 | 8 | 8  | 10 | 6 | 6  | 4  | 6  | 6  | 8  | 6  |
| 6  | 6 | 6  | 6 | 6  | 6  | 6 | 6  | 6  | 8 | 8  | 6  | 6  | 6  | 8  | 10 |
| 8  | 6 | 10 | 6 | 6  | 6  | 6 | 6  | 8  | 6 | 8  | 6  | 8  | 6  | 6  | 8  |
| 6  | 8 | 6  | 6 | 8  | 6  | 8 | 8  | 6  | 6 | 6  | 8  | 6  | 6  | 8  | 6  |

Max DP Value for Proposed S-box-1: 10  
Max DP Value for Proposed S-box-2: 10  
Max DP Value for Proposed S-box-3: 10

**Table 13**

LP for Proposed S-boxes.

| Linear Approximation Probability: | Max Count | Max Value |
|-----------------------------------|-----------|-----------|
| LP for proposed S-box-1           | 164       | 0.140625  |
| LP for proposed S-box-2           | 160       | 0.125     |
| LP for proposed S-box-3           | 162       | 0.13281   |

### 5.5. Linear approximation probability

Linear approximation probability (LP) is one of the most important tests in order to design and analysis of S-boxes. An S-box's resistance to linear cryptanalysis attacks is gauged by its LP. The S-box is less vulnerable to this kind of attack if the LP value is higher. As a result, it is essential to design S-boxes with high values for LP in order to ensure the

security of cryptographic systems (see Table 13). The total number of input and output bits that are coincident is used to calculate LP. The following is the mathematical formula to calculate the LP.

$$LP_{(a,b)} = (2^{n-1} + 1)^{-1} \times |\{x : S(x) \oplus S(x \oplus a) = b\}| \quad (9)$$

Where  $a$  and  $b$  are input and output differences respectively and  $n$  is a bit-length of the input and output.

### 5.6. Bijectivity

Bijectivity is the capacity for each input value to be specifically mapped to a specific output value and vice versa. The S-box's bijectivity is essential for the security of the encryption algorithm because it guarantees that the encryption process is reversible and that no data is lost. Our proposed S-boxes are bijective when their nonlinearity results

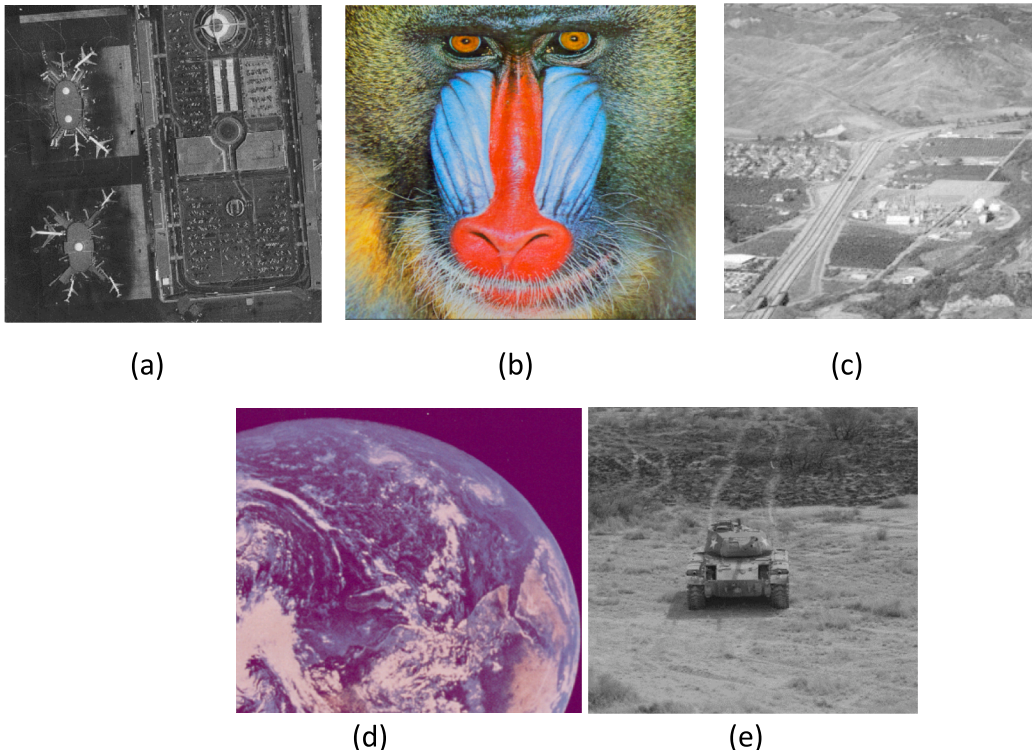


**Fig. 3.** Set of plain images (a-e) of Airport, Baboon, chemical plant, earth space, and Tank to examine image encryption algorithm.



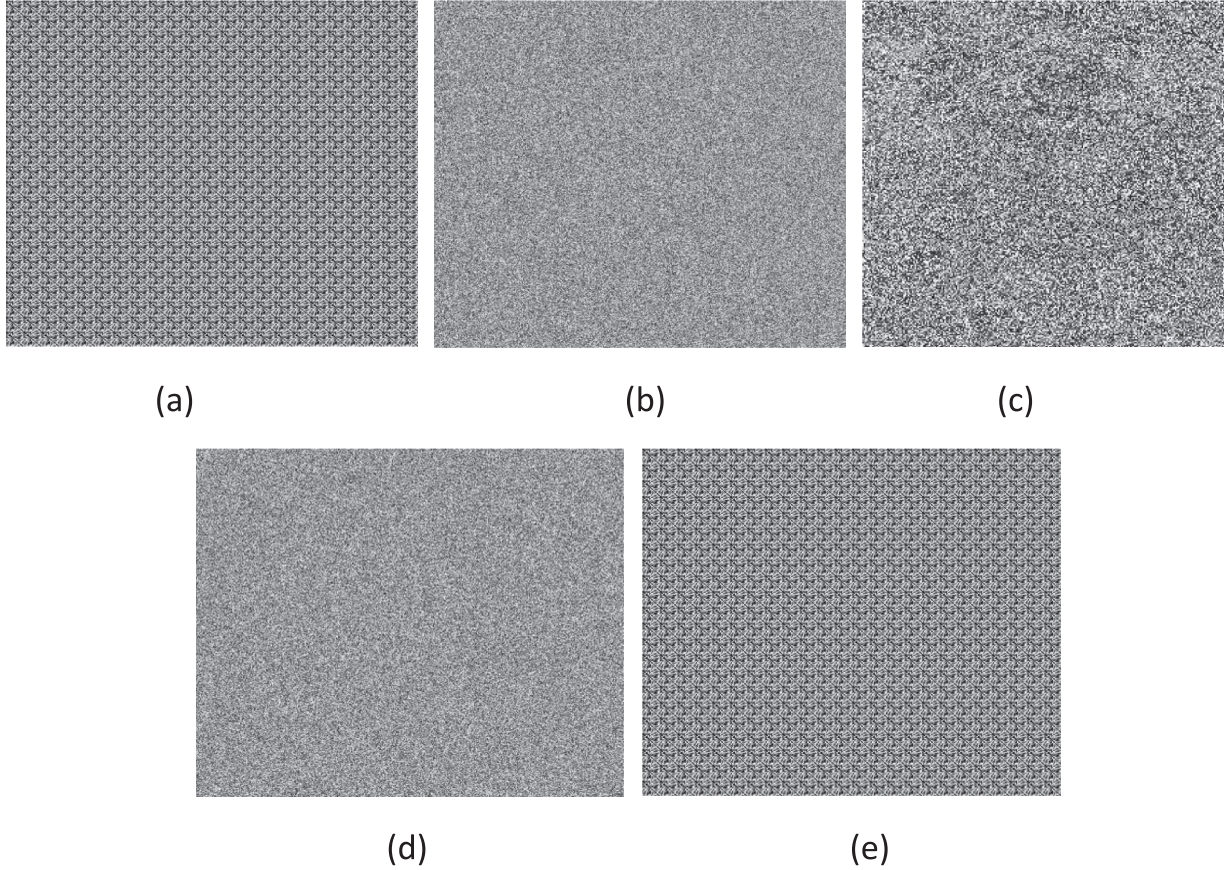


Fig. 4. Set of Encrypted images (a-e) of Airport, Baboon, chemical plant, earth space, and Tank.

are greater than or equal to 112.

## 6. Analysis of cryptographic properties of an encrypted image

The performance and security attributes of the proposed chaotic-based S-box encryption scheme is assessed through a number of experimental tests. These tests are set up and run on a Windows 10 desktop with a Core i5 processor, 8 GB of RAM, and the MATLAB 2020a platform. Standard RGB and grayscale images (airport, a baboon, a chemical plant, an earthly space, and a tank) are included in the experiment, which are chosen from the USC-SIPI image dataset. Figs. 3 and 4 provide an illustration of these experimental images .

### 6.1. Correlation analysis

Images may be subject to security breaches during transmission or storage due to the high degree of correlation between adjacent pixels. As a result, encryption techniques for images therefore aim to reduce this correlation to conceal image content. It measures the correlation between adjacent pixels and has a range of  $-1$  to  $1$ . No correlation is indicated by a value of  $0$ , maximum positive correlation is represented by a value of  $1$ , and maximum negative correlation is indicated by a value of  $-1$ . The correlation coefficients between adjacent pixels in a cipher image can be minimized to produce low correlation values, which denote higher security.

The correlation of adjacent pixels can be calculated as:

$$CC_v = \frac{\sum_{i=1}^{H-1} \sum_{j=1}^w (C_{(i,j)} - \bar{C})(C_{(i+1,j)} - \bar{C})}{\sqrt{\sum_{i=1}^{H-1} \sum_{j=1}^w (C_{(i,j)} - \bar{C})^2 \sum_{i=1}^{H-1} \sum_{j=1}^w (C_{(i+1,j)} - \bar{C})^2}} \quad (9)$$

This equation presented in this context employs the width and height

Table 14

The correlation coefficients of different images.

| Correlation Coefficient |             |           |            |             |
|-------------------------|-------------|-----------|------------|-------------|
| Image                   | Size        | Vertical  | Horizontal | Diagonal    |
| 1. Airport              | 1024 × 1024 | 0.037239  | 0.039534   | 0.072504    |
| 2. Baboon               | 512 × 512   | 0.0036625 | 0.0030674  | −0.0017916  |
| 3. Chemical Plant       | 256 × 256   | 0.0030192 | 0.0045205  | 0.0051687   |
| 4. Earth Space          | 512 × 512   | 0.0010803 | 0.0036398  | −0.00012869 |
| 5. Tank                 | 512 × 512   | 0.089371  | 0.017622   | 0.0088644   |

of an image as  $W$  and  $H$ , respectively. The adjacent pixel values of the cipher image at positions  $(i+1, j)$  and  $(i, j)$  are represented by  $C(i+1, j)$  and  $C(i, j)$ , respectively. The below mathematical expression is used to calculate the correlation coefficient between plaintext and its corresponding cipher image:

$$CC_{P,C} = \frac{\sum_{i=1}^H \sum_{j=1}^w (P_{(i,j)} - \bar{P})(C_{(i,j)} - \bar{C})}{\sqrt{\sum_{i=1}^H \sum_{j=1}^w (P_{(i,j)} - \bar{P})^2 \sum_{i=1}^H \sum_{j=1}^w (C_{(i,j)} - \bar{C})^2}} \quad (10)$$

This equation uses the width and height of the images, which are denoted here by the letters  $W$  and  $H$ , respectively. According to Table 14, the proposed algorithm exhibits low correlation values between the plaintext and cipher images. This implies a high level of security because it suggests there is little similarity or predictability between the original message and the encrypted image.

### 6.2. Entropy analysis

Entropy is used to evaluate the degree of uncertainty and randomness in image. It is widely used in communication system to specify the

**Table 15**  
Entropy Results.

| Entropy Analysis |                |         |
|------------------|----------------|---------|
| Image            | Color and Size | Entropy |
| Airport          | 1024 × 1024    | 7.9     |
| Baboon           | 512 × 512      | 7.7     |
| Chemical Plant   | 256 × 256      | 7.3     |
| Earth Space      | 512 × 512      | 7.7     |
| Tank             | 512 × 512      | 7.8     |

**Table 16**  
Homogeneity Results.

| Homogeneity    |                |             |
|----------------|----------------|-------------|
| Image          | Color and Size | Homogeneity |
| Airport        | 1024 × 1024    | 0.37297     |
| Baboon         | 512 × 512      | 0.46778     |
| Chemical Plant | 256 × 256      | 0.40667     |
| Earth Space    | 512 × 512      | 0.46884     |
| Tank           | 512 × 512      | 0.37137     |

amount of information in a message. The probability distribution of the pixel values in the encrypted image can be used to estimate the entropy. A higher level of randomness among pixels indicates that the image is more secure against attacks. Mathematically it is represented as:

$$H(k) = - \sum_{i=0}^{2^n-1} p(k_i) \log_2 p(k_i) \quad (11)$$

In this Equ. (11) H represent entropy which measure in bits, and  $p(k_i)$  shows the probability of  $k_i$  and  $i$  represents the intensity of the probability. Mathematically local entropy is represented as:

$$H_{K,T_B}(S) = \sum_{i=1}^K \frac{H(S_i)}{K} \quad (12)$$

The calculated entropy values for the proposed algorithm are more significant and close to the ideal entropy (see Table 15).

### 6.3. Homogeneity

Homogeneity analysis in image processing is a technique that assesses how closely a gray-level co-occurrence matrix (GLCM) conforms to its diagonal. The GLCM is a helpful tool for feature and texture extraction because it measures the frequency of adjacent horizontal pixels with gray-level values of  $i$  and  $j$ . The resulting homogeneity value ranges from 0 to 1, its lower values reflect better performance.

Mathematically, the homogeneity is calculated as follow: (see Table 16)

$$Homogeneity = \sum_{i,j} \frac{p(i,j)}{1 + |i - j|} \quad (13)$$

The aforementioned equation determines the value of a given GLCM element, where  $i$  and  $j$  are two adjacent gray-level values. Table 16 shows the results of the homogeneity of different images and the proposed algorithm give low values of homogeneity.

### 6.4. Contrast

Contrast analysis is a technique for comparing the variations between a pixel and its neighboring pixels of an entire image. The lightest and darkest areas of an image are referred to this technique. The difference between the light and dark portions is significant in high contrast images. if an image has high contrast, it is considered more secure because it suggests a higher level of randomness. It is represented as:

**Table 17**  
Contrast Results.

| Image          | Color and Size | Contrast |
|----------------|----------------|----------|
| Airport        | 1024 × 1024    | 0.097598 |
| Baboon         | 512 × 512      | 0.038494 |
| Chemical Plant | 256 × 256      | 0.084479 |
| Earth Space    | 512 × 512      | 0.038193 |
| Tank           | 512 × 512      | 0.097193 |

**Table 18**  
Energy Results.

| Image          | Color and Size | Energy     |
|----------------|----------------|------------|
| Airport        | 1024 × 1024    | 2.57488231 |
| Baboon         | 512 × 512      | 6.3908717  |
| Chemical Plant | 256 × 256      | 1.5926979  |
| Earth Space    | 512 × 512      | 6.3966082  |
| Tank           | 512 × 512      | 6.3096318  |

$$Contrast = \sum_{i,j} |i - j|^2 p(i,j) \quad (14)$$

Table 17 shows the results of the contrast of different images and the proposed algorithm give high contrast levels in encrypted images.

### 6.5. Energy

Energy, also referred to as uniformity, is a metric that assesses the total squared values in an image's Grey-Level Co-occurrence Matrix (GLCM). A cipher image with a lower energy value is preferred because it is more secure. The energy metric typically has a range of 0 to 1. The mathematical formula for calculating energy is as follows:

$$Energy = \sum_{i,j} p(i,j)^2 \quad (15)$$

Where  $i$  and  $j$  represent two levels of brightness that appear side-by-side horizontally in an image. Table 18 shows the results of the energy of different images by the proposed algorithm.

### 6.6. Histogram analysis

A fundamental method for processing images, histogram analysis involves analyzing and interpreting the distribution of pixels in an image. A histogram is a useful tool for analyzing an image's overall brightness, contrast, and tonal distribution because it plots the frequency of pixel intensities against the corresponding intensity values. Common methods derived from histogram analysis include thresholding, contrast stretching, and histogram equalization, which allow for the enhancement, normalization, and segmentation of images. Additionally, histogram analysis is essential for many applications, including image recognition, object detection, and medical imaging.

The following Fig. 5 shows the histogram distribution of the original images:

The following Fig. 6 shows the histogram distribution of the encrypted images:

Based on the analysis, the histogram analysis provides valuable insights into the frequency distribution of images and highlights the presence of distinct peaks, suggesting the presence of multiple groups or subpopulations within the image.

## 7. Discussion and comparative analysis

In our work, various performance metrics are used to evaluate the encryption security provided by the proposed algorithm for an input image. 1-D and 2-D chaotic maps are mathematical models that exhibit

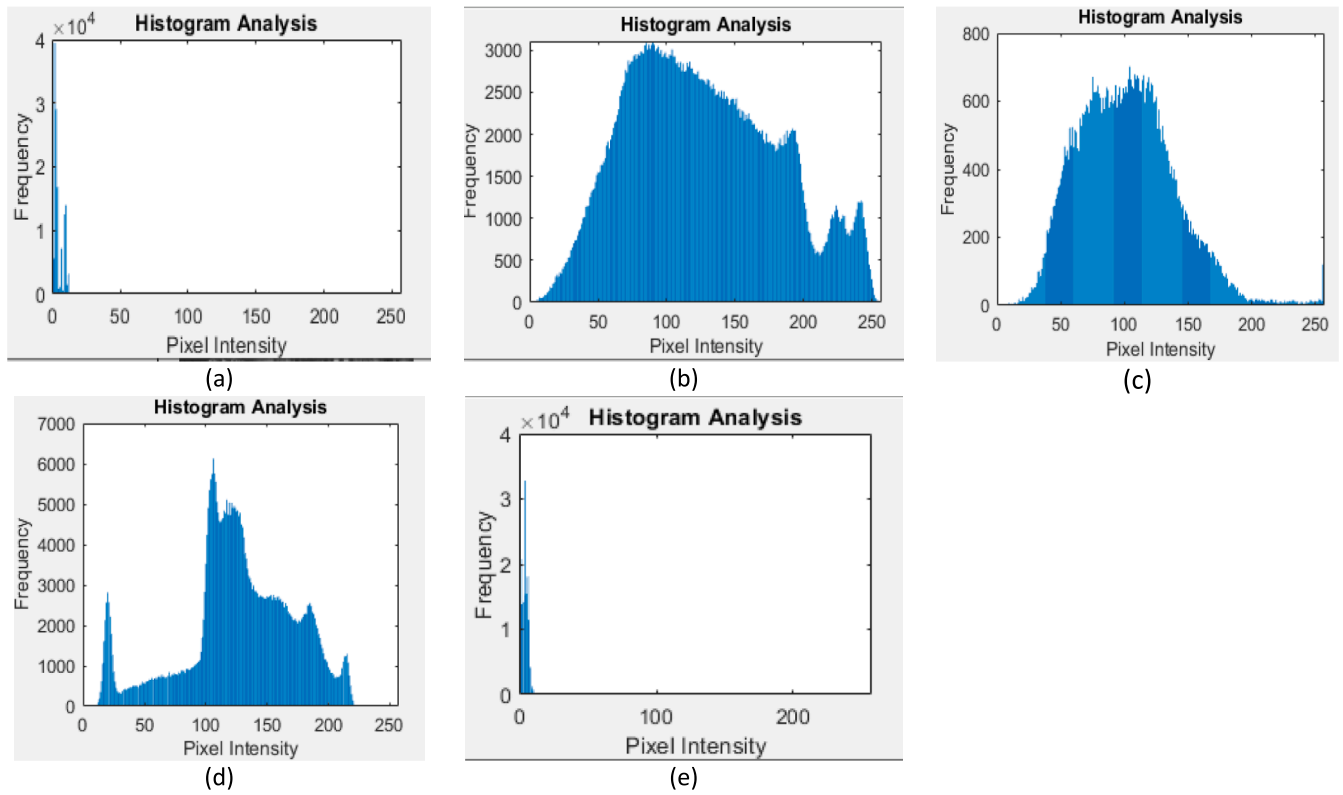


Fig. 5. Histogram of plain images.

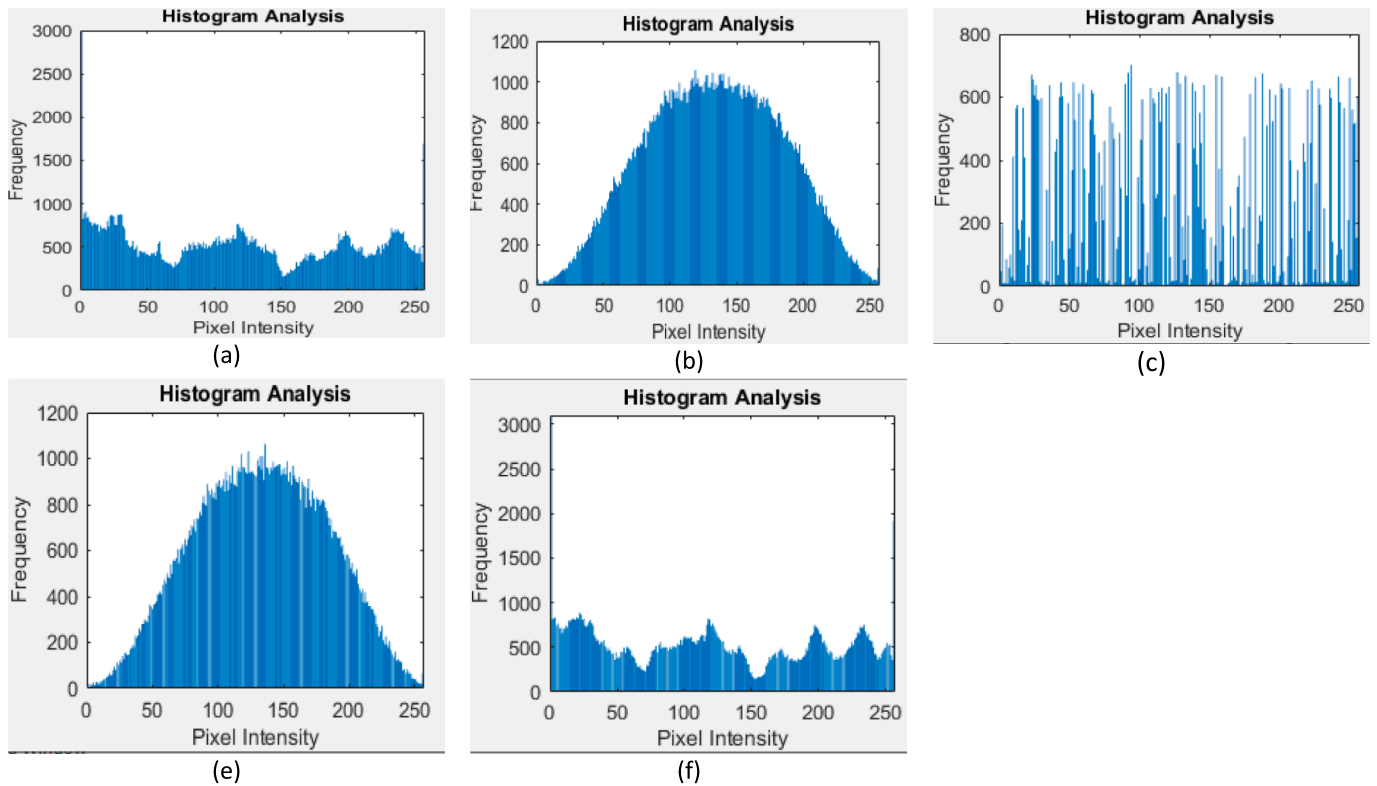


Fig. 6. Histogram Analysis of Encrypted Images.

chaotic behavior. In comparison to 2-D chaotic maps, 1-D chaotic maps are typically easier to compute and analyze [42]. As a result, several attacks can be used against the low-dimensional chaos-based image

encryption scheme [43]. The proposed encryption scheme uses 2-D chaotic systems. A variety of test cases are run on a set of color and grayscale images and in our case entropy value approaches to 8, which



**Table 19**  
Comparative Analysis of Proposed Image Encryption Algorithm.

| Sr. No. | Encryption Schemes Presented in Literature   | Proposed Image Encryption Algorithm  |
|---------|--|--|
| 1       | Most of the techniques presented in the literature are specific to certain types of images, with some designed for greyscale images and others for RGB images. | The proposed algorithm offers greater practical flexibility by supporting a wide variety of image formats and color representations, including greyscale and RGB images.   |
| 2       | The outdated encryption methods used by the old algorithms may be vulnerable to attacks and have security flaws.   | The proposed algorithm includes sophisticated cryptographic mechanisms that guarantee a higher level of security and resistance to various encryption-breaking techniques. |
| 3       | The outdated algorithm might not be able to keep up with new demands for image encryption or changing security threats.  | The proposed algorithm is intended to be adaptable, enabling simple updates and improvements to counter new vulnerabilities and address changing encryption requirements.  |
| 4       | The outdated algorithm might not be sufficiently resilient, making it vulnerable to widely used attacks like statistical analysis or brute force.              | The novel algorithm incorporates strong encryption methods that increase its resistance to known attacks and offer improved security for the encrypted images.             |
| 5       | Most researchers only use a few security analysis measures.  | Different metric measures such as Entropy, Contrast, Correlation, homogeneity, and energy are taken into account for results and analysis.                                 |

**Table 20**  
Notation Table.

| Notation   | Notation Name              | Description   |
|------------|----------------------------|---|
| S-box      | Substitution Box           | An S-box is a core component of block ciphers.  |
| NL         | Nonlinearity               | Used to make a complex relationship between input and output.                               |
| SAC        | Strict Avalanche Criterion | Used to measure the sensitivity of an algorithm to small changes in its input.              |
| BIC        | Bit Independence Criterion | When only one input bit is changed, two output bits should change regardless of each other. |
| DP         | Differential Probability   | Used to evaluate the security against differential cryptanalysis.                           |
| LP         | Linear Probability         | Used to evaluate the security against linear cryptanalysis.                                 |
| $\nu$      | Nu                         | Parameter in chaotic map.   |
| $\mu$      | Mu                         | Variable in mathematical equations.   |
| $\tau$     | Tau                        | Variable or parameter in mathematical equations.  |
| $\epsilon$ | Epsilon                    | Parameter to represent the behavior of functions.   |

indicates presented encryption algorithm is robust and strong.

Similarly, the proposed algorithm exhibits low correlation values between the plaintext and cipher images. This implies a high level of security because it suggests there is little similarity or predictability between the original image and the encrypted image.

In the same way, the analysis section also presents robust findings with satisfactory energy and homogeneity results. The energy analysis shows that computational resources are used effectively during the encryption process, resulting in optimal performance with minimal waste. Additionally, the achieved homogeneity in the encrypted images exhibits a desired degree of uniformity in the distribution of pixel values. This consistency points to a strong encryption algorithm that successfully scrambles the image data while maintaining a reliable and aesthetically pleasing output.

Additionally, the proposed encryption scheme places less computational strain on the system than the high-dimensional chaotic sequence. Table 19 displays the results obtained from the experimental measurements of several standard images using various existing methods, including the model we have proposed. The proposed encryption

method is notable for its ability to function well on both RGB and greyscale images (see Table 20).

8. Conclusion

In this study, we propose three chaotic S-boxes based on the Zaslavsky map, Henon map, and Baker’s map, which have nonlinearities of 113.75, 114.25, and 112, respectively. We thoroughly examine these S-boxes using cryptographic tests, including nonlinearity, strict avalanche criterion, bit independence criterion, linear approximation probability, differential approximation probability, and bijectivity. The results of these tests are satisfactory and meet our expectations. Additionally, we propose an image encryption algorithm based on our novel S-boxes. To assess the strength and performance of our proposed scheme, we perform statistical tests, including entropy, correlation, homogeneity, energy, and contrast. The experimental results demonstrate that our scheme has good robustness against differential attacks.

Declaration of Competing Interest

The authors declare that they have no known competing financial interests or personal relationships that could have appeared to influence the work reported in this paper. Moreover, this article is a part of the PhD thesis "Design and Optimization of Nonlinear Component of Block Cipher: Applications to Multimedia Security" submitted to NUML, Pakistan.

References

[1] Chai X, Fu X, Gan Z, Lu Y, Chen Y. A color image cryptosystem based on dynamic DNA encryption and chaos. *Signal Process* 2019;155:44–62. <https://doi.org/10.1016/j.sigpro.2018.09.029>.

[2] Chai X, Zhi X, Gan Z, Zhang Y, Chen Y, Fu J. Combining improved genetic algorithm and matrix semi-tensor product (STP) in color image encryption. *Signal Process* 2021;183. <https://doi.org/10.1016/j.sigpro.2021.108041>.

[3] Wang L, Cao Y, Jahanshahi H, Wang Z, Mou J. Color image encryption algorithm based on Double layer Josephus scramble and laser chaotic system. *Optik (Stuttg)* 2023;275. <https://doi.org/10.1016/j.ijleo.2023.170590>.

[4] Alexan W, Alexan N, Gabr M. Multiple-Layer Image Encryption Utilizing Fractional-Order Chen Hyperchaotic Map and Cryptographically Secure PRNGs. *Fractal Fract* 2023;7. <https://doi.org/10.3390/fractalfract7040287>.

[5] Waheed A, Subhan F, Suud MM, Alam M, Ahmad S. An analytical review of current S-box design methodologies, performance evaluation criteria, and major challenges. *Multimed Tools Appl* 2023. <https://doi.org/10.1007/s11042-023-14910-3>.

[6] Guan ZH, Huang F, Guan W. Chaos-based image encryption algorithm. *Phys Lett Sect A Gen At Solid State Phys* 2005;346:153–7. <https://doi.org/10.1016/j.physleta.2005.08.006>.

[7] Alexan W, Elbeltagy M, Aboshousha A. RGB Image Encryption through Cellular Automata, S-Box and the Lorenz System. *Symmetry (Basel)* 2022;14. <https://doi.org/10.3390/sym14030443>.

[8] Bian J, Tao Y, Wang Z, Dong Y, Li Z, Zhao X, et al. A true random number generator based on double threshold-switching memristors for image encryption. *Appl Phys Lett* 2023;122. <https://doi.org/10.1063/5.0145875>.

[9] Liang Q, Zhu C. A new one-dimensional chaotic map for image encryption scheme based on random DNA coding. *Opt Laser Technol* 2023;160. <https://doi.org/10.1016/j.optlastec.2022.109033>.

[10] Zhao W, Chang Z, Ma C, Shen Z. A Pseudorandom Number Generator Based on the Chaotic Map and Quantum Random Walks. *Entropy* 2023;25. <https://doi.org/10.3390/e25010166>.

[11] Das D, Pradhan C. Image Encryption Based on Cyclic Chaos, PRNG and Arnold’s Cat Map. *Lect Notes Networks Syst* 2023;572:281–91. [https://doi.org/10.1007/978-981-19-7615-5\\_25](https://doi.org/10.1007/978-981-19-7615-5_25).

[12] Alexan W, Chen YL, Por LY, Gabr M. Hyperchaotic Maps and the Single Neuron Model: A Novel Framework for Chaos-Based Image Encryption. *Symmetry (Basel)* 2023;15. <https://doi.org/10.3390/sym15051081>.

[13] Waheed A, Subhan F, Suud MM, Malik YH, Al E. Construction of nonlinear component of block cipher using coset graph. *AIMS Math* 2023;8:21644–67. <https://doi.org/10.3934/math.20231104>.

[14] Wang J, Yang Y, Wang T, Simon Sherratt R, Zhang J. Big data service architecture: A survey. *J Internet Technol* 2020;21:393–405. <https://doi.org/10.3966/160792642020032102008>.

[15] Zhang J, Zhong S, Wang T, Chao HC, Wang J. Blockchain-based Systems and Applications: A survey. *J Internet Technol* 2020;21:1–14. <https://doi.org/10.3966/160792642020012101001>.

[16] Bu HH, Kim NC, Park KW, Kim SH. Content-based image retrieval using combined texture and color features based on multi-resolution multi-direction filtering and

- color autocorrelogram. *J Ambient Intell Humaniz Comput* 2019. <https://doi.org/10.1007/s12652-019-01466-0>.
- [17] Liu C, Li K, Li K, Buaya R. A New Service Mechanism for Profit Optimizations of a Cloud Provider and Its Users. *IEEE Trans Cloud Comput* 2021;9:14–26. <https://doi.org/10.1109/TCC.2017.2701793>.
- [18] Lu L, Ren X, Yeh KH, Tan Z, Chanussot J. Exploring coupled images fusion based on joint tensor decomposition. *Human-Centric Comput. Inf Sci* 2020;10. <https://doi.org/10.1186/s13673-020-00215-z>.
- [19] Hamza R, Titouna F. A novel sensitive image encryption algorithm based on the Zaslavsky chaotic map. *Inf Secur J* 2016;25:162–79. <https://doi.org/10.1080/19393555.2016.1212954>.
- [20] Chaos and Cryptography. Baker's map || Generate chaotic keys || Generate prime numbers [Video] 2021.
- [21] Chaos and Cryptography. PRNG with Zaslavsky Map || Pseudo Random Number Generator [Video] 2021.
- [22] Chaos and Cryptography. Generation to chaotic values of Henon Map || 2D chaotic map [Video] 2021.
- [23] Abduljabbar ZA, Abduljaleel IQ, Ma J, Sibahee MAA, Nyangaresi VO, Honi DG, et al. Provably Secure and Fast Color Image Encryption Algorithm Based on S-Boxes and Hyperchaotic Map. *IEEE Access* 2022;10:26257–70. <https://doi.org/10.1109/ACCESS.2022.3151174>.
- [24] Guisande N, Di Nunzio MP, Martinez N, Rosso OA, Montani F. Chaotic dynamics of the Hénon map and neuronal input-output: A comparison with neurophysiological data. *Chaos* 2023;33. <https://doi.org/10.1063/5.0142773>.
- [25] Alhumyani H. Dual Image Cryptosystem Using Henon Map and Discrete Fourier Transform. *Intell Autom Soft Comput* 2023;36:2933–45. <https://doi.org/10.32604/iasc.2023.034689>.
- [26] Abd-El-Atty B. Efficient S-box construction based on quantum-inspired quantum walks with PSO algorithm and its application to image cryptosystem. *Complex Intell Syst* 2023. <https://doi.org/10.1007/s40747-023-00988-7>.
- [27] Zhu D, Tong X, Zhang M, Wang Z. A new s-box generation method and advanced design based on combined chaotic system. *Symmetry (Basel)* 2020;12:1–17. <https://doi.org/10.3390/sym12122087>.
- [28] Zahid AH, Iliyasu AM, Ahmad M, Shaban MMU, Arshad MJ, Alhadawi HS, et al. A Novel Construction of Dynamic S-Box with High Nonlinearity Using Heuristic Evolution. *IEEE Access* 2021;9:67797–812. <https://doi.org/10.1109/ACCESS.2021.3077194>.
- [29] Alghafis A, Munir N, Khan M. An encryption scheme based on chaotic Rabinovich-Fabrikant system and S8 confusion component. *Multimed Tools Appl* 2021;80:7967–85. <https://doi.org/10.1007/s11042-020-10142-x>.
- [30] Jiang Z, Ding Q. Construction of an s-box based on chaotic and bent functions. *Symmetry (Basel)* 2021;13. <https://doi.org/10.3390/sym13040671>.
- [31] Dimitrov MM. On the Design of Chaos-Based S-Boxes. *IEEE Access* 2020;8:117173–81. <https://doi.org/10.1109/ACCESS.2020.3004526>.
- [32] Shahzad I, Mushtaq Q, Razaq A. Construction of New S-Box Using Action of Quotient of the Modular Group for Multimedia Security. *Secur Commun. Networks* 2019;2019. <https://doi.org/10.1155/2019/2847801>.
- [33] Hua Z, Li J, Chen Y, Yi S. Design and application of an S-box using complete Latin square. *Nonlinear Dyn* 2021;104:807–25. <https://doi.org/10.1007/s11071-021-06308-3>.
- [34] Javeed A, Shah T, Attaullah. Design of an S-box using Rabinovich-Fabrikant system of differential equations perceiving third order nonlinearity. *Multimed Tools Appl* 2020;79:6649–60. <https://doi.org/10.1007/s11042-019-08393-4>.
- [35] Ali TS, Ali R. A novel color image encryption scheme based on a new dynamic compound chaotic map and S-box. *Multimed Tools Appl* 2022;81:20585–609. <https://doi.org/10.1007/s11042-022-12268-6>.
- [36] Hematpour N, Ahadpour S, Behnia S. Presence of dynamics of quantum dots in the digital signature using DNA alphabet and chaotic S-box. *Multimed Tools Appl* 2021;80:10509–31. <https://doi.org/10.1007/s11042-020-10059-5>.
- [37] Nizam Chew LC, Ismail ES. S-box construction based on linear fractional transformation and permutation function. *Symmetry (Basel)* 2020;12. <https://doi.org/10.3390/SYM12050826>.
- [38] Artuğer F, Özkaynak F. SBOX-CGA: substitution box generator based on chaos and genetic algorithm. *Neural Comput Appl* 2022. <https://doi.org/10.1007/s00521-022-07589-4>.
- [39] Panchami V, Mathews MM. A Substitution box for Lightweight Ciphers to Secure Internet of Things. *J King Saud Univ - Comput Inf Sci* 2023. <https://doi.org/10.1016/j.jksuci.2023.03.004>.
- [40] Cheng R, Zhou Y, Miao X, Hu J. Analysis of a New Improved AES S-Box. *Structure* 2023;109–25. [https://doi.org/10.1007/978-3-031-30623-5\\_8](https://doi.org/10.1007/978-3-031-30623-5_8).
- [41] Webster AF, Tavares SE. On the Design of S-Boxes. *Lect Notes Comput Sci (Including Subser Lect Notes Artif Intell Lect Notes Bioinformatics)* 1986;218 LNCS:523–34. [https://doi.org/10.1007/3-540-39799-X\\_41](https://doi.org/10.1007/3-540-39799-X_41).
- [42] Zhou S, Wei Y, Zhang Y, Teng L. Novel Chaotic Image Cryptosystem Using Dynamic DNA Coding 2022.
- [43] Solak E, Çokal C, Yildiz OT, Biyikoğlu T. Cryptanalysis of Fridrich's chaotic image encryption. *Int J Bifurc Chaos* 2010;20:1405–13. <https://doi.org/10.1142/S0218127410026563>.